

# Modulated structure of $\text{Ag}_2\text{SnO}_3$ studied by high-resolution electron microscopy

Takeo Oku,<sup>a†</sup> Anna Carlsson,<sup>a</sup>  
Jan-Olov Bovin,<sup>a</sup> Christer  
Svensson,<sup>a</sup> L. Reine  
Wallenberg,<sup>a\*</sup> Christoph Linke<sup>b</sup>  
and Martin Jansen<sup>c</sup>

<sup>a</sup>National Center for HREM, Inorganic Chemistry 2, Chemical Center, Lund University, PO Box 124, S-221 00 Lund, Sweden, <sup>b</sup>University of Bonn, Gerhard-Domagk-Strasse 1, D-53121 Bonn, Germany, and <sup>c</sup>Max-Planck-Institut für Festkörperforschung, Heisenbergstrasse 1, D-70569 Stuttgart, Germany

† Present address: Institute of Scientific and Industrial Research, Osaka University, Mihogaoka 8-1, Ibaraki, Osaka 567-0047, Japan.

Correspondence e-mail:  
reine.wallenberg@oorg2.lth.se

The modulated structure of  $\text{Ag}_2\text{SnO}_3$ , disilver tin trioxide, was investigated by high-resolution electron microscopy and electron diffraction along four different directions. Electron diffraction showed an incommensurate one-dimensional modulated structure with a modulation wavevector of  $1/6.4a^*$ . High-resolution images showed a large number of superstructure domains with the size range 10–100 nm and orientations related by hexagonal rotation. The modulation was determined to be displacements along the  $c$  axis of the Ag atoms both in octahedral and linear coordination. An approximate structure model with a commensurate sixfold superstructure, with an orthorhombic cell ( $P2_12_12_1$ ,  $a = 2.922$ ,  $b = 1.267$ ,  $c = 0.562$  nm), is proposed. Calculated images and electron diffraction patterns, based on this model, agree well with experimental observations.

Received 28 June 1999

Accepted 25 October 1999

## 1. Introduction

Ag-based oxides are expected to show a variety of structures and properties, owing to the  $d^{10}$  cation configuration in the crystal (Jansen, 1987). Crystals of  $\text{Ag}_2\text{SnO}_3$  have been recently synthesized and the average structure ( $P6_322$ ,  $a = 0.56230$ ,  $c = 1.26694$  nm) was determined by X-ray diffraction (Linke & Jansen, 1997). The atomic coordinates are listed in Table 1. The structure is related to that of delafossite,  $\text{CuFeO}_2$  (Linke & Jansen, 1997). There are two types of Ag atom sites in the unit cell. One is in the pure silver layers (Ag1), and the other is within the tin oxide layers (Ag2) with octahedral coordination. In the refined model the Ag atoms in the tin oxide layers take three equally occupied positions,  $\sim 0.08$  nm apart along the  $c$  axis. However, additional reflections along the  $a^*$  direction were observed, indicating a modulated structure.

The purpose of the present work is to investigate the modulated structure of  $\text{Ag}_2\text{SnO}_3$  by high-resolution electron microscopy (HREM) and electron diffraction. To enable a direct comparison of digital data, a slow-scan CCD camera was used for recording the HREM images (Oku *et al.*, 1998). The modulation amplitude could be determined by direct recording of silver and tin atom positions by HREM.

## 2. Experimental

$\text{Ag}_2\text{SnO}_3$  crystals were prepared by solid-state reaction of freshly prepared  $\text{K}_2\text{Sn}(\text{OH})_6$  and  $\text{Ag}_2\text{O}$  at 703 K and under an oxygen pressure of 350 bar (Linke & Jansen, 1997). The  $\text{Ag}_2\text{SnO}_3$  crystals were analyzed by a scanning electron microscope (JSM-840A) with an energy-dispersive X-ray

**Table 1**

Structural parameters for  $\text{Ag}_2\text{SnO}_3$  (Linke & Jansen, 1997).

Space group  $P6_322$ ,  $a = 0.56230$  and  $c = 1.26694$  nm.

	$x$	$y$	$z$	Occupancy	$B^*$ ( $\text{nm}^2$ )
Ag1	0.3259	0	0	1.0	0.031
Ag2	0.6667	0.3333	0.1845	0.3333	0.030
Ag3	0.6667	0.3333	0.25	0.3333	0.038
Sn1	0.3333	0.6667	0.25	1.0	0.014
Sn2	0	0	0.25	1.0	0.017
O	0.0511	0.3343	0.1621	1.0	0.029

spectrometer to determine the elemental composition of Ag and Sn in the crystal. Samples for HREM observations were prepared by dispersing crushed material on a holey carbon grid. HREM observations were performed with a 400 kV electron microscope (JEM-4000EX) with a resolution of 0.16 nm. The electron microscope was equipped with a slow-scan CCD camera (Gatan SSC model 694). The area of detection of the CCD camera is  $1024 \times 1024$  pixels with a pixel size of  $24 \times 24 \mu\text{m}$ . The images were recorded at a magnification of  $1\,000\,000 \times$ . For image processing of the recorded HREM images, Digital Micrograph (Gatan Inc. Pleasanton,

**Table 2**

Parameters used for HREM image calculations.

Parameter	Value
Accelerating voltage (kV)	400
Spherical aberration $C_s$ (mm)	1.0
Radius of the objective aperture ( $\text{nm}^{-1}$ )	6.3
Focus spread (nm)	8.0
Semi-angle of convergence (mrad)	0.55

CA, USA) and Semper (Synoptics Ltd, Cambridge, England) software was used. As a first step, the digital images were masked and fast Fourier transformed. The reciprocal lattice was indexed according to a sixfold commensurate unit cell and the lattice parameters were determined using the positions of the strongest peaks in the transform. The local background was subtracted and the amplitudes and phases of the peaks were corrected using symmetrization (Hovmöller *et al.*, 1984; Carlsson, 1992). Before correcting the phases, the phase origin was determined by investigating the origin shift that gave the best accordance with the phase conditions for the two-dimensional plane group. Averaged symmetrized images were reconstructed from the corrected Fourier transforms. HREM

images were calculated by the multi-slice method (Cowley & Moodie, 1957) using the MacTempas (Total Resolution, CA, USA) software and compared to experimental images in order to verify the suggested model. The microscope parameters used in the image calculations are listed in Table 2.

### 3. Results and discussion

Electron diffraction patterns recorded along (a) [001], (b)  $[\bar{1}13]$ , (c) [010] and (d)  $[1\bar{1}0]$  directions of the subcell of  $\text{Ag}_2\text{SnO}_3$  are shown in Fig. 1. Apart from the fundamental reflections, a large number of additional diffraction spots are observed in Figs. 1(b)–(d). Fig. 1(b) was recorded from the same region as in Fig. 1(a), but after tilting ( $14.4^\circ$ ). Extra reflections appear around the fundamental reflections in Fig. 1(b) and are also visible in (c) and (d). Streaks are observed along the  $c^*$  axis in Figs. 1(c) and (d), because of stacking faults along the  $c$  axis.

Enlarged electron diffraction patterns along the  $[\bar{1}13]$  and [010] directions of  $\text{Ag}_2\text{SnO}_3$  are shown in Figs. 2(a) and (b), respectively. In Fig. 2(b), the extra reflections are located with a separating distance of

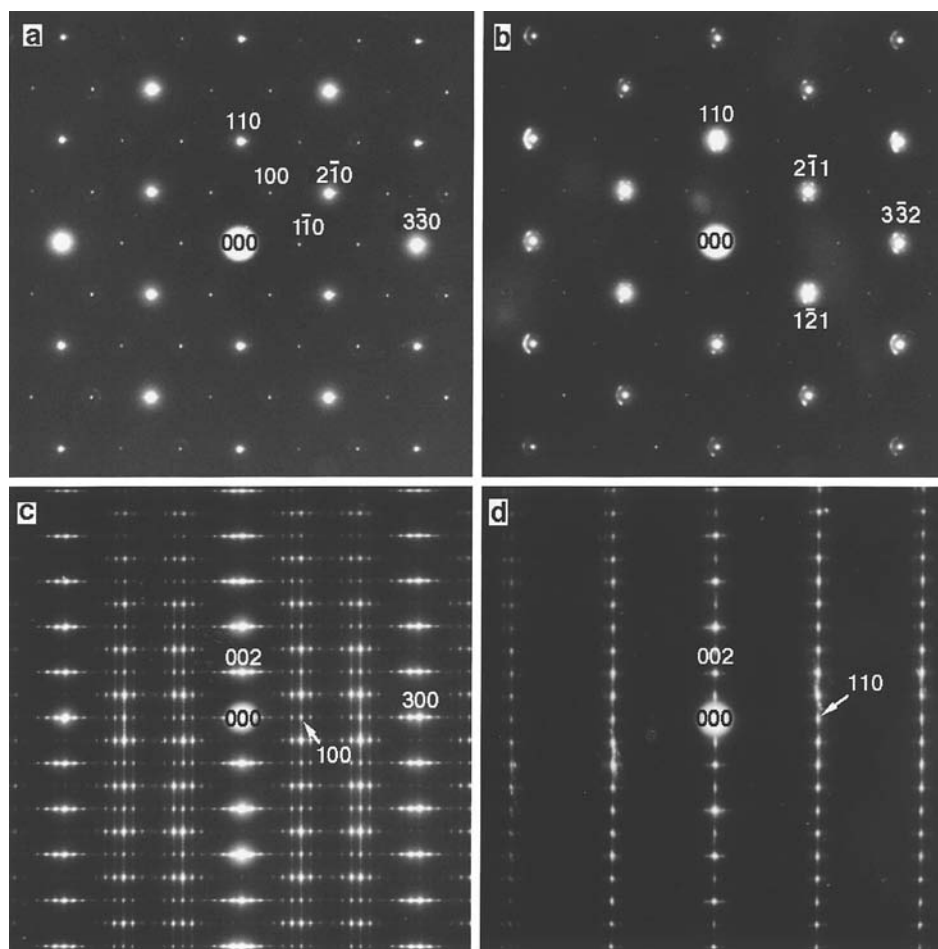


**Figure 1**

Electron diffraction patterns recorded along (a) [001], (b)  $[\bar{1}13]$ , (c) [010] and (d)  $[1\bar{1}0]$  directions of  $\text{Ag}_2\text{SnO}_3$ . Indices according to cell determined by X-ray diffraction.

$\sim 1/6a^*$  along the  $a^*$  direction, corresponding to a 3.1 nm period. However, the third-order satellites do not coincide, as shown by the arrows. The modulation wavevector is determined as  $1/6.4a^*$ , which indicates an incommensurately modulated structure. Fig. 2(a) also shows satellite reflections, observed along the three directions indicated by the arrows.

In HREM images of  $\text{Ag}_2\text{SnO}_3$ , recorded slightly off the [001] direction, modulated structure domains can be seen with sizes in the range between 10 and 100 nm, as shown in Fig. 3. The image is taken along the  $[\bar{1}13]$  direction, which corresponds to the diffraction pattern of Fig. 2(a). Within each domain, a one-dimensional modulation with a period of  $\sim 3$  nm can be observed and this occurs in three distinct directions. Therefore, a diffraction pattern from a 'large' area ( $>100$  nm) along the  $[\bar{1}13]$  direction should show three sets of satellite spots, as shown in Fig. 2(a).

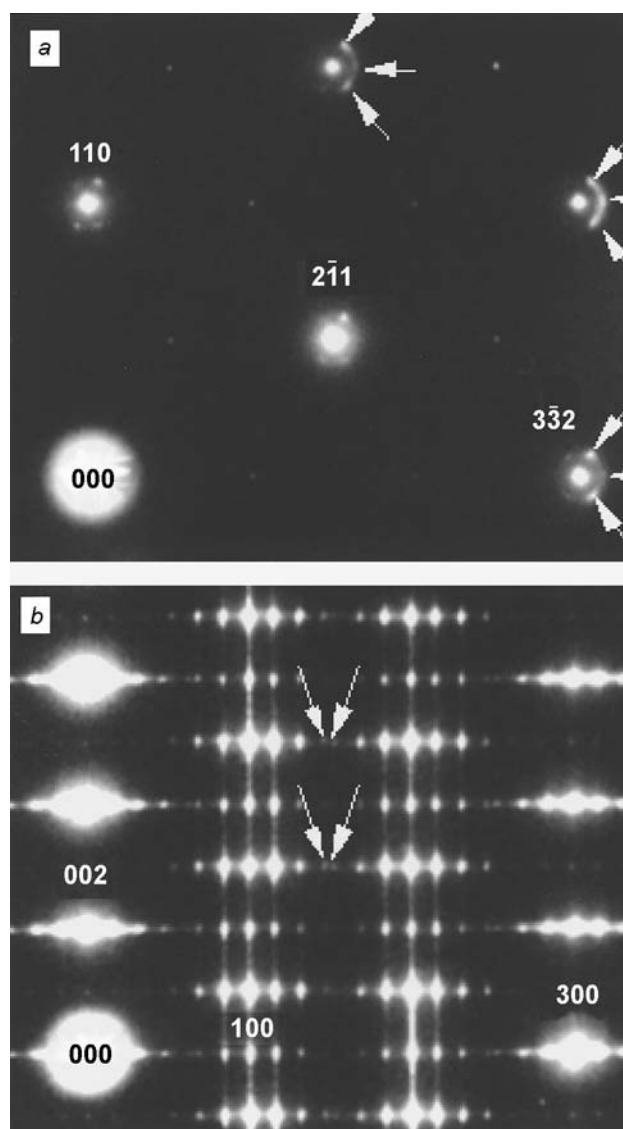


**Figure 2**  
Enlarged electron diffraction patterns of (a)  $[\bar{1}13]$  and (b) [010] directions of  $\text{Ag}_2\text{SnO}_3$ .

Fig. 4(a) is an HREM image with [010] incidence, corresponding to the electron diffraction pattern of Fig. 1(c). The image shows modulation contrast with a period of  $\sim 3$  nm along the projected [100] direction. Based on the high-reso-

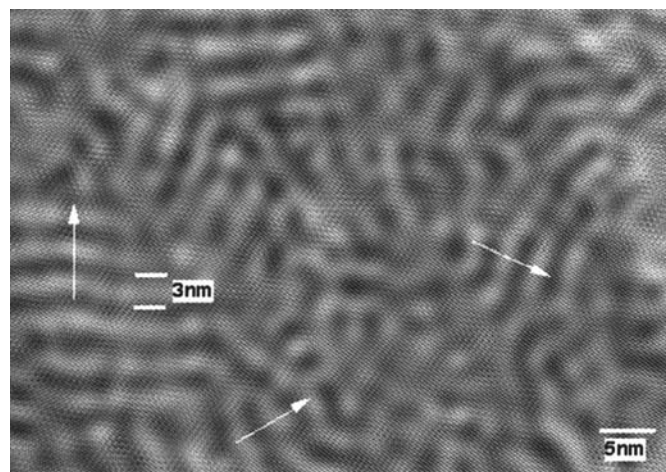


**Figure 3**  
Processed experimental HREM image recorded along the  $[\bar{1}13]$  direction of  $\text{Ag}_2\text{SnO}_3$ .

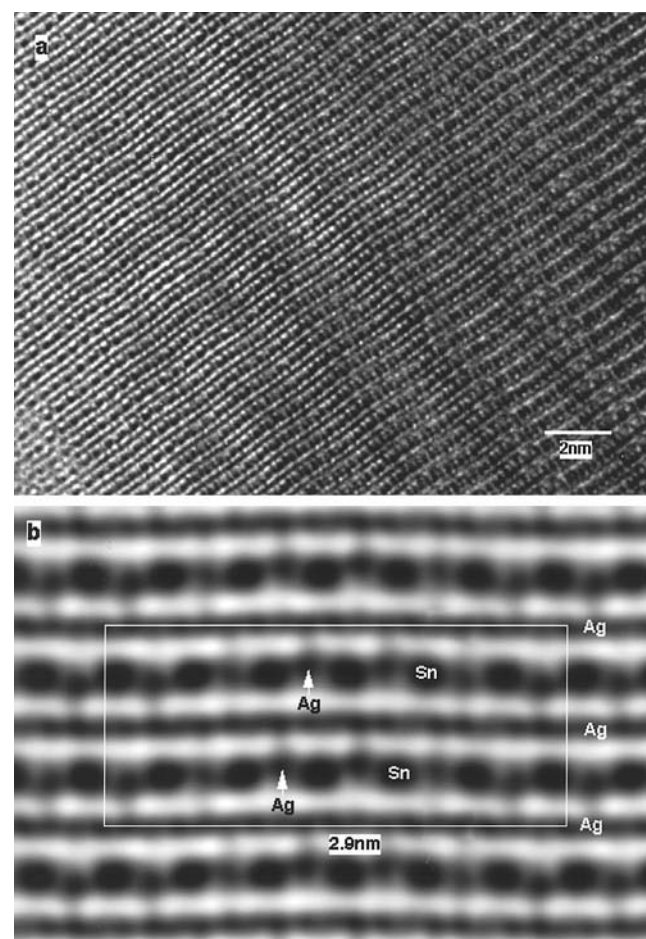


**Figure 4**  
(a) HREM image taken along the [010] direction of  $\text{Ag}_2\text{SnO}_3$ . (b) Averaged and symmetrized image of (a).

**Table 3**  
Structural parameters for modulated structure of  $\text{Ag}_2\text{SnO}_3$ .

Space group  $P2_12_12_1$ ,  $a = 2.922$ ,  $b = 1.267$  and  $c = 0.562$  nm. All occupancy factors 1.0.  $B$  (isotropic displacement parameter) values for Ag10–12 are a weighted average of the X-ray parameters.

	$x$	$y$	$z$	$B$ ( $\text{nm}^2$ )
Ag1	0.1667	0.4925	0.4241	0.031
Ag2	0.3333	0.0075	0.5759	0.031
Ag3	0.4457	0.0140	0.5871	0.031
Ag4	0	0.4851	0.9241	0.031
Ag5	0.0543	0.4860	0.4130	0.031
Ag6	0.3877	0.0144	0.0871	0.031
Ag7	0.2790	0.0026	0.0871	0.031
Ag8	0.2210	0.4974	0.9130	0.031
Ag9	0.1124	0.4886	0.9130	0.031
Ag10	0.3889	0.2761	0.75	0.033
Ag11	0.2222	0.2239	0.25	0.033
Ag12	0.0556	0.1978	0.75	0.033
Sn1	0.3333	0.25	0.25	0.017
Sn2	0	0.25	0.25	0.017
Sn3	0.1667	0.25	0.75	0.017
Sn4	0.2778	0.25	0.75	0.014
Sn5	0.1111	0.25	0.25	0.014
Sn6	0.4444	0.25	0.25	0.014
O1	0.0557	0.3379	0.3661	0.029
O2	0.3890	0.3379	0.3661	0.029
O3	0.2223	0.1621	0.6340	0.029
O4	0.2223	0.3379	0.8661	0.029
O5	0.3891	0.1621	0.1340	0.029
O6	0.0557	0.1621	0.1340	0.029
O7	0.3248	0.1621	0.5588	0.029
O8	0.1581	0.3379	0.4413	0.029
O9	0.4915	0.3379	0.4413	0.029
O10	0.2861	0.3379	0.4427	0.029
O11	0.1195	0.1621	0.5573	0.029
O12	0.4528	0.1621	0.5573	0.029
O13	0.1582	0.1621	0.0588	0.029
O14	0.3248	0.3379	0.9413	0.029
O15	0.2861	0.1621	0.0573	0.029
O16	0.4528	0.3379	0.9427	0.029
O17	0.4915	0.1621	0.0588	0.029
O18	0.1195	0.3379	0.9427	0.029

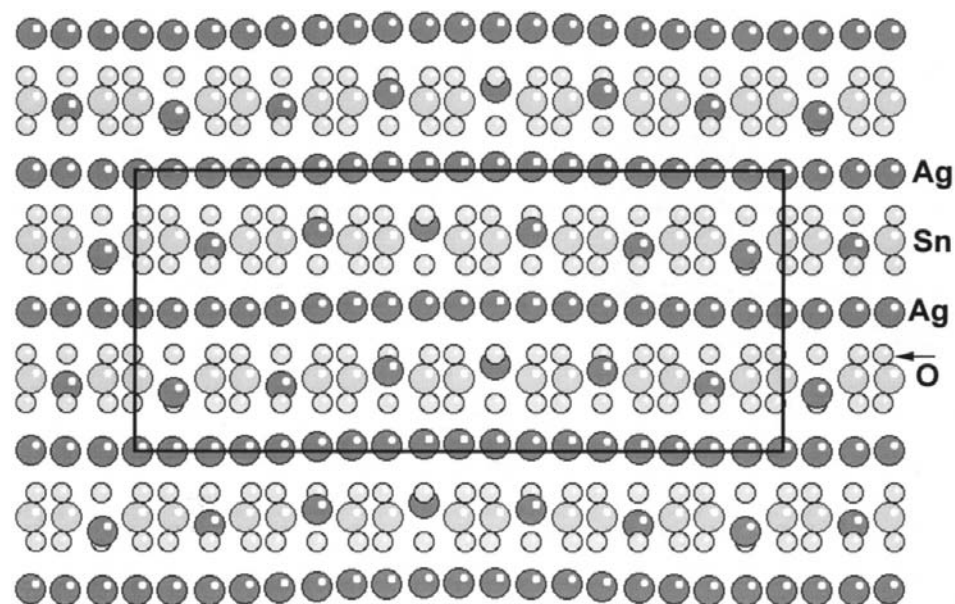


**Figure 5**  
Structure model for the commensurate superstructure with an orthorhombic cell ( $P2_12_12_1$ ,  $a = 2.922$ ,  $b = 1.267$ ,  $c = 0.562$  nm), viewed along  $[001]$ .

lution images, image processing was carried out under the assumption of a commensurate structure with a period six times that of the subcell along the  $[100]$  direction. The new unit cell is orthorhombic with cell parameters  $a = 6 \cdot a_H \cdot \cos 30^\circ = 2.922$ ,  $b = c_H = 1.267$ ,  $c = b_H = 0.562$  nm, where subscript  $H$  denotes the hexagonal subcell. It is drawn with white lines in Fig. 4(b), which is a projection along the orthorhombic  $[001]$  direction. Under optimal conditions, the atomic coordinates can be directly estimated from HREM images (Oku *et al.*, 1995; Weirich *et al.*, 1996; Oku & Nakajima, 1998). In Fig. 4 large and small black dots correspond to Sn and Ag atoms, respectively. A sinusoidal displacement of Ag atoms along the hexagonal  $c$ -axis in both the tin oxide and pure silver layers is clearly observed. From this image, the coordinates of Ag atoms were directly estimated from the local image intensity minimum and a model for the modulated structure was constructed, where the remaining Sn and O atoms were derived from the X-ray model (Fig. 5). From the relationships between the atomic coordinates of the superstructure model, the space group  $P2_12_12_1$  could be derived. A list of atomic coordinates is given in Table 3.

The atomic ratio of Ag/Sn was determined to be 2.1:1.0 by scanning electron microscopy with energy dispersive X-ray analysis, which is within experimental error of the previous X-ray results. These results suggest that the modulation is not a compositional modulation, but rather an atomic displacement modulation.

In the present model, the sinusoidal displacements of Ag atoms in the  $\text{SnO}_2$  and Ag layers have amplitudes along the  $c$  axis of 0.0661 and 0.0189 nm, respectively. In fractional coordinates the waves can be described by  $y_1 = y_1^o - 0.0522\sin(2\pi x_1 + \pi/2)$  and  $y_2 = y_2^o - 0.0149\sin(2\pi x_2 + 7\pi/18)$ . In the X-ray results (unit cell and coordinates listed in Table 1), the Ag2 and Ag3 atoms in the  $\text{SnO}_2$  layer also occupy a distribution of positions along the hexagonal  $c$  axis, revealed by the elongated electron density distribution, and corresponding to an amplitude of  $\sim 0.083$  nm. However, the minor displacements of Ag1 found here could not be observed in the X-ray work.

High-resolution images, based on the suggested structure model, were calculated along  $[001]$  of the orthorhombic cell with the defocus value of  $-50$  nm (optimum defocus) and a crystal thickness of 2.2 nm (Fig. 6, see also Table 2). The displacements of Ag atoms in the  $\text{SnO}_2$  and Ag layers along the  $c$  axis can be clearly observed. This calculated image agrees well with the processed image of Fig. 4(b) and is also consistent with the smeared electron density in the X-ray structure which gives rise to three Ag

positions with 1/3 occupancy each, but in too close proximity of each other to be physically correct.

Fig. 7 shows calculated electron diffraction patterns of the proposed model along four different directions. These directions correspond to those of Fig. 1. In the calculated patterns

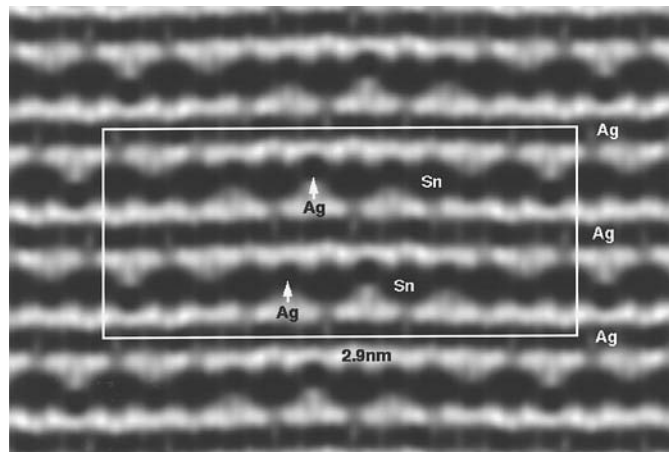


**Figure 6**  
Calculated HREM image along [001] based on the structure model of Fig. 5.

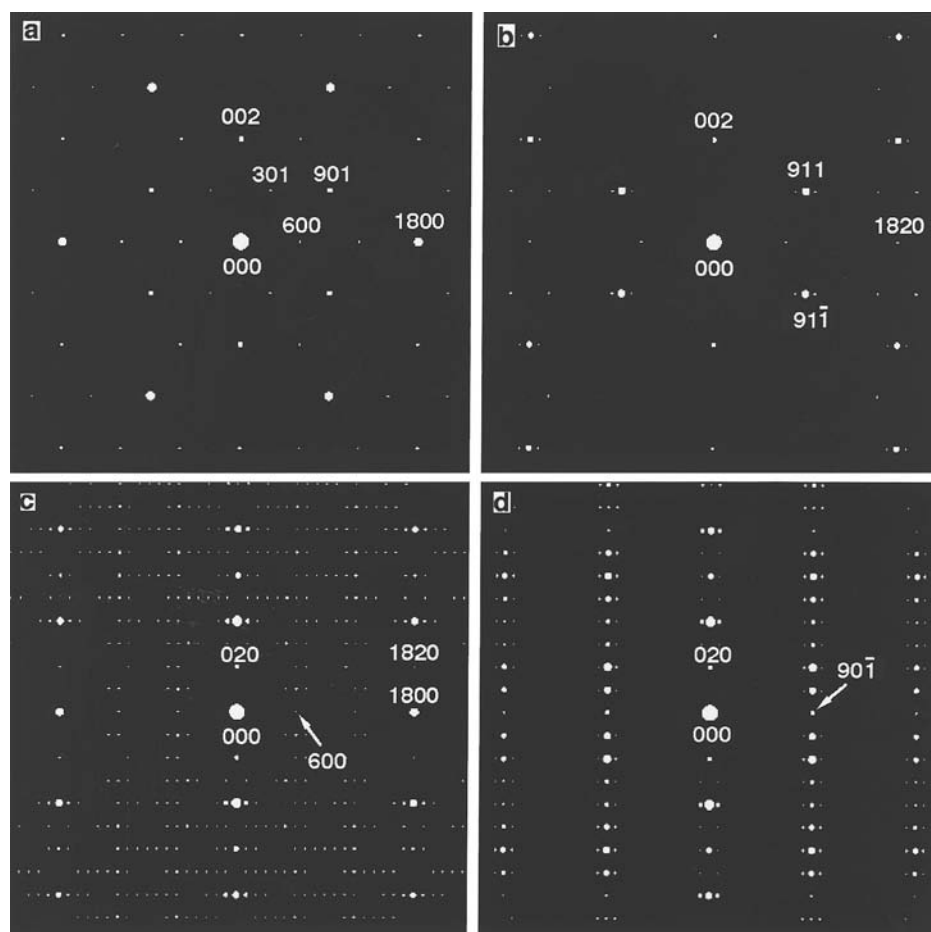


**Figure 7**  
Calculated electron diffraction patterns along (a) [010], (b)  $[\bar{1}90]$ , (c) [001] and (d) [109] directions of the superstructure of  $\text{Ag}_2\text{SnO}_3$ , based on the structure model in Fig. 5.

in Figs. 7(b)–(d), the extra reflections due to the modulation of the structure are clearly observed. Extra reflections are not observed in Fig. 7(a), since the displacements of Ag atoms are only along the  $c$  axis. The fundamental diffraction spots in the calculated and observed diffraction patterns agree very well. The calculated extra reflections owing to the modulated structure also agree reasonably well with the experimental ones, with only minor discrepancies. The small difference for the satellite reflections in the diffraction patterns, recorded along [001] and [109], could be due to the crystal thickness and stacking faults, and to the hexagonal twinning in the observed patterns. In Fig. 1(b) only, the three sets of extra reflections, which are due to the domain structure, are simultaneously visible. The model corresponds to one of these directions. Further structure analysis of the modulated structure by single-crystal X-ray diffraction is in progress.

#### 4. Conclusions

The modulated structure of  $\text{Ag}_2\text{SnO}_3$  was investigated by direct observation of Ag and Sn atom positions in HREM images, and examination of satellite reflections in electron diffraction patterns recorded along several directions of the crystal. The primary wavevector of the one-dimensional modulation was determined to be  $1/6.4a^*$ , which indicates an incommensurately modulated structure. Superstructure domains with sizes in the range 10–100 nm were observed in three directions in high-resolution images recorded along  $[\bar{1}13]$ . Direct determination of the metal-atom positions from HREM image contrast showed that the modulation is one displacement of Ag atoms along the  $c$  axis in both  $\text{SnO}_2$  and Ag layers. Assuming a commensurate superstructure with a period of six times that of the subcell along the [100] direction, an orthorhombic structure model of the modulation was proposed ( $P2_12_12_1$ ,  $a = 6 \cdot a_H \cos 30^\circ = 2.922$ ,  $b = c_H = 1.267$ ,  $c = b_H = 0.562$  nm, where subscript  $H$  denotes the hexagonal subcell). The calculated HREM images and electron diffraction patterns based on the structure model agree well with the experimental data and explain the X-ray average structure model. We have chosen to use this approximate commensurate description based on the electron diffraction and HREM imaging, and left the incommensurate superspace description to future X-ray work. A full, reliable statement of extinction conditions

without multiple scattering effects would require convergent beam analysis of very small areas, preferably with tilting around systematic rows to cut off dynamic routes.

The authors would like to acknowledge Christer Jönsson for help with SEM-EDX analysis and Ulrich Häussermann for translations. This work was supported by the Swedish Natural Science Research Council.

### References

- Carlsson, A. (1992). *Proc. European Congress on Electron Microscopy*, Spain, p. 497.
- Cowley, J. M. & Moodie, A. F. (1957). *Acta Cryst.* **10**, 609–619.
- Hovmöller, S., Sjögren, A., Farrants, G., Sundberg, M. & Marinder, B.-O. (1984). *Nature*, **331**, 238–241.
- Jansen, M. (1987). *Angew. Chem. Int. Ed. Engl.* **26**, 1098–1110.
- Linke, C. & Jansen, M. (1997). *Z. Anorg. Allg. Chem.* **623**, 1441–1446.
- Oku, T., Carlsson, A., Wallenberg, L. R., Malm, J.-O., Bovin, J.-O., Higashi, I., Tanaka, T. & Ishizawa, Y. (1998). *J. Solid State Chem.* **135**, 182–193.
- Oku, T. & Nakajima, S. (1998). *J. Mater. Res.* **13**, 1136–1140.
- Oku, T., Shindo, D., Nakajima, S., Tokiwa, A., Kikuchi, M., Syono, Y. & Hiraga, K. (1995). *Nova Sci. Pub.* **15**, 103–144.
- Weirich, T. E., Ramlau, R., Simon, A., Hovmöller, S. & Zou, X. (1996). *Nature*, **382**, 144–146.